IDRiM (2025) 15 (1) ISSN: 2185-8322
DOI10.5595/001c.129129

Journal of Integrated Disaster Risk Management

Regular Article

Flooding Probability in Temporal Risk Assessment for LNG Vaporizer Unit established in West Coast Malaysia

Cengiz Dirik[1*], Dayang Radiah Binti Biak[2], Musab Bin Abdul Razak[2] and Nik Nor Liyana Nik Ibrahim[2]

Received: 28/07/2023 / Accepted: 25/11/2024 / Published online: 31/01/2025

Abstract In the Liquid Natural Gas (LNG) processing field, accidents can be caused by various natural occurrences. Lightning and flooding scenarios are common triggering agents for industrial accidents, and there is a chance that LNG units could sustain significant damages in such an event. This study integrates these two natural phenomena into the temporal model and analysis. The principle of temporal failure has been applied to an LNG`s SCV (Submerged Combustion Vaporizer) unit affected by floods and lightning, which are considered correlated natural phenomena. This work proves and applies a new dimension (temporal) to risk analysis in chemical process safety engineering for the first time. As a result of the simulation, Sequential (Temporal) failures 1, 2, and 3 comprise 31.25%, 47.9%, and 13.5% of the total failures, respectively, and together make up 92.65% of the total failures, which cannot be detectable by conventional approaches. Meanwhile, classical failures contribute to only 6.8% of the total failures. For a safety-critical system, these values are crucial. Using Monte Carlo Simulation (MCS), we provide information on the occurrence of failures for the vaporizer based on operational hours. From the results, the vaporizer can be expected to fail 29 times over 300,000 service hours, with only 2 of these being conventional failures. After total failure frequency was obtained Event Tree Analysis (ETA) was performed, and negative consequence probability was found 3.25x10-6(/h).

Keywords: dynamic fault tree, temporal fault tree, reliability, flooding, Monte Carlo simulation

[1] Department of Chemical and Environmental Engineering, Faculty of Engineering, Safety Engineering Interest Group, Universiti Putra Malaysia, Malaysia

[2] Department of Chemical and Environmental Engineering, Faculty of Engineering, Universiti Putra Malaysia, Malaysia

* Corresponding author email: gs52238@student.upm.edu.my

1. INTRODUCTION

A SCV unit utilizes a burner combustion system as a heat source. SCVs are designed to rapidly increase the temperature of LNG (−160 ◦C) to ambient temperatures; in brief, it allows for a temperature increase and require a quick start-up or shut-down. Steam from the combustion products condenses into liquid water after LNG vaporization, releasing a significant amount of latent heat (Han et al., 2018). Studies have shown that the ice layer's enormous thermal resistance, which affects the vaporizer's ability to evaporate gas efficiently, is still the biggest problem (Pan et al., 2020). Thus, the SCV vaporizer system typically may present a high risk of failure among LNG processing units. In addition, some notable accidents occurred in the LNG purification and regeneration system on March 31, 2014, at the Plymouth-Liquefied Natural Gas (LNG) Peak Shaving Plant, which had a catastrophic malfunction, resulting in an explosion. The breakdown started in the pipework that heated the gas for adsorber regeneration between the salt bath heater and the adsorber vessel (Rukke & Katchmar, 2016).

Lightning is a key factor leading to malfunctions, failures, and fire incidents (Dirik et al., 2022), especially when considering storage tanks that store volatile chemicals (Garcia et al., 2013). More than 70% of power outages in Malaysia are caused by lightning. A certain number of lightning strikes being followed by flooding is the main concern of this study. Thus, the sequential failure structure of probability of the lightning–flooding formation is proposed, in order to capture the temporal failure. Moreover, ongoing global climate change has been observed, which is expected to lead to more extreme precipitation accompanied by intensification of the occurrence and severity of flood events (Winsemius et al., 2016; Ricci et al., 2021; Sofia & Nikolopoulos, 2020; Papadopoulos et al., 2009). In addition, most severe climatic incidents are related to flooding events (Gungle & Krider, 2006; Tapia et al., 1998) have discussed the relationship between cloud-to-ground (CG) lightning and surface rainfall on the east coast of central Florida. From their research results, they drew the conclusion that "the optimum lag time versus the total number of CG flashes shows a linear trend (R2 = 0.56). With a linear fit to the lagged rain volume vs. the number of concurrent CG flashes (R2 = 0.83), it is concluded that lightning and flash flood probability have a linear correlation. Thus, this relationship can be formulated and simulated in process safety risk analysis."

Some papers on flooding prediction in Malaysia, such as that of Ahmad et al. (2022), have captured 63 positive CG flashes close to the lightning measurement system in Malacca. They reported that "all positive CG flashes were detected within four hours. The occurrence of positive CG flashes on the day when the flash flood happened in Malacca on October 20, 2021, has been analyzed. It has been found that the flash flood event between 15:30 and 16:30 in Malacca was closely correlated with the large number of positive CG flashes detected." An important factor relating to these two phenomena is that they occur sequentially; thus, when one occurs, the other event can be expected to follow. This is the key idea underlying the concept of temporal failure. This study took this correlation number "63, "which was implemented into temporal fault probability (Ismail, 2019). Some flood risk assessment studies, such as Ismail (2019), have determined the characteristics of real flooding events in Malaysia. They concluded that: (i) "The average flood water level in Peninsular Malaysia is 0.3, 0.6, and 1.0 m for various types of flooding in Malaysia" (the reason why it is important to know the depth of flooding that pumps, electrical parts, and so on, may be installed on the ground. If the depth of the flood can reach their sensitive parts, it may lead to additional risk; thus, the depth of the flood may cause additional failures); (ii) "the average flash flood occurs in less than 6 h in most locations, but flash floods may exceed more than 6 h with the flood water level above 1.0 m due to heavy rain and high tidal level;" and (iii) "the average flood duration for monsoon floods is two days, with an average flood water level of 1.0 m, depending on rainfall conditions", so these parameters can be taken as temporal parameters. (Ismail, 2019).

Another paper has studied the correlation between lightning and precipitation in Northern Malaysia and proposed combining the effect of lightning and flooding risks (Mohammad et al., 2019). It tabulated flash rates for three hours, with a maximum of 73 and a minimum of 65 flashes occurring over a 15-minute period, and integrated the obtained values into a research system for failure analysis. Another study has supported the existence of a correlation between flooding and lightning density (Johari et al., 2021). The authors observed positive CG in the northern prefecture of Malaysia, tabulated the geometric mean of each year's number of average strikes, and found that positive CG constituted only 1.6% of the total CG flashes. They also observed that "the occurrence of positive CG follows the weather pattern of Malaysia, with a strong connection between positive CG and rain events. Most positive CG occurred in November, while the least occurred in February. Each year's average flash count is about 190,760 times in Shah Alam prefecture" (Ab-Kadir, 2016). One hundred seventy-two lightning ground flash records were presented, with 57 flashes of positive lightning per km2 a year and high numbers of subsequent return strokes. The data were recorded in November 2013 at the Universiti Putra Malaysia (UPM; 2◦59j19.9jj N, 101◦43j 29.8jj E) in Serdang. Previous studies, such as Ab-Kadir (2016), Ahmad et al. (2022), Mohammad et al. (2019), Ismail (2019), Johari et al. (2021), have proposed correlation parameters and lightning strike density values for Selangor prefecture, which were implemented into the system simulation proposed in this paper using Visual studio-based C# coding.

Similar studies regarding other geographic locations, such as Price et al. (2011), have shown that lightning strike density and flooding probability are linearly correlated, so lightning data can significantly help estimate rainfall. The significant finding of this study was that "Since lightning data are available in close to real-time and cover large regions, lightning can be used to produce warnings for the public and local and regional governments about thunderstorm activity in the next few hours." It has been demonstrated that the calculation of rainfall from satellite data may be greatly improved by lightning data. According to (Papadopoulos et al., 2009) lightning data may be utilized to provide alerts for local and regional governments about impending thunderstorm activity because they are readily available in close to real-time and cover huge territories. The research by Price et al. (2011) shown that "lightning data could be assimilated into extreme rainy prediction models to improve the initial conditions of the models, hence improving the 1-2 day forecasts of heavy precipitation and flash floods." Zorilla (2011) has suggested a geo-lightning grid-based strategy that prioritizes places based on their importance for public safety. A geographic information system was used to create the geo-lightning grid. He discussed a power system case study and showed how lightning may affect the system.

The most frequent natural catastrophes in Malaysia are flooding and lightning, which happen more often during the monsoon season. "The coasts of peninsular Malaysia are the most prone to flooding," according to Ismail (2019), "especially during the northeast monsoon season from October to March. The major goal of pertinent prior research was to evaluate the frequency, duration, and intensity of flash floods in northern Malaysia.

The main goal of this work is to simulate at the regional scale and analyze the lightning-flooding correlation patterns. The proposed study aims to use the correlation between lightning and flooding to develop a system failure simulation model that considers the temporal effects of lightning and flooding on the total system. This is a very new area in chemical process safety study. A Temporal Fault Tree Analysis (TFTA) has been previously developed by the authors, and sequential failures of systems in the process industry that function under the PAND gate concept were assessed (Dirik et al., 2022). The specificity of this study is that it emphasizes the combined effects of natural phenomena (i.e., lightning and flooding events) to assess the sequential failure probability. This study is mainly comprised of two parts. The first part considers the influence of the temporal timing of natural disasters on the vaporizer unit and temporal risk prediction; for this part, we provide a detailed data analysis. The second part involves conventional failure probability calculations for repairable and unrepairable parts.

2. METHODOLOGY

We analyzed data that had previously been collected by The Offshore and Onshore Reliability Data (OREDA) project, which was established in 1981 in cooperation with the Norwegian Petroleum Directorate (now Petroleum Safety Authority Norway). It is an important reliability data source for the oil and gas industry (Wingender, 1986), OREDA Handbooks provide reliability data for process equipment. It provides three categories of data, that is, inventory part, failure part, and maintenance part for each equipment (Mannan, 2012). (e.g., in national statistics, official records archives, publications, and previous studies).

The failure data were fitted to a Weibull distribution to obtain the Weibull parameter, which was later utilized to calculate the total failure of the system based on the described failure conditions. The component failure data categorization is provided in Figure 1.

Table 1 and 2 are arranged according to the categorization presented in Figure 1, where Table 1 provides the shape factor (β) values for various components. Preventive maintenance may help to extend the service years of aging units before they are worn out; however, a preventive

DOI10.5595/001c.129129

maintenance schedule or assessment was not included in the considerations of the used failure data. These data can assist relevant facility owners in preparing a suitable plan for preventative maintenance of such systems.

Among all the unrepairable components that are present in LNG SCV systems, the level sensors and manifold presented the highest failure rates (or the shortest mean time to fail).

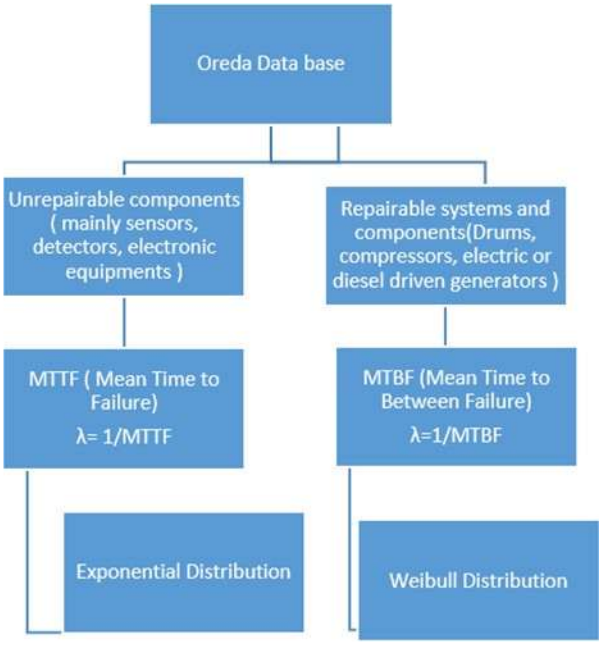

Figure 1. OREDA data type categorization

Table 1 shows the repairable system obeys the Weibull distribution, while Table 2 presents data obtained for the components using an exponential distribution.

The failure rate of a component or system can be expressed as the probability per unit time that a component or system will experience a failure at that time. Unrepairable components obey an exponential distribution.

After obtaining the component data, we studied another input for the system failure analysis: lightning strike data. We consider that, if the number of lightning strikes is above a certain threshold, flooding will consequently occur. This sequence is important for system temporal failure detection. Not only the lightning–flooding sequence but also the lightning strike itself, may lead to the malfunction or failure of the sensors which detect failure, thus activating the ESD system. Following temporal logic, the lightning strike (and/or the induced magnetic field) may first cause 4/6 sensor failure.

Lightning parameters for north Malaysia were obtained from previous studies and included in the system MCS.

DOI10.5595/001c.129129

Table 1. Weibull parameters for repairable components (Dirik et al., 2022)

No	Component	Weibull Parameter	
		α (Hour)	(β)
1	Centrifugal pump (CP)	479,842	1.0095
2	Lift non-return valve (LRV; Swing Check Valve)	1,999,448	0.95
3	Swing check valve (SCV)	1,999,448	0.95
4	Globe valve (GV)	3,149,282	0.99
5	Butterfly valve (BV)	333,624	1.093
6	Butterfly Emergency Shut Down (ESD) Valve (BVAE)	61,345	2.78
7	Butterfly Process Control valve	436,073	1.91
8	Control Valve (CV)	454,020	3.18
9	High-Pressure Compressor	196,237.6	0.51
10	BOG Compressor	85,019	2.21
11	Relief Valve (RV)	1,620,619	1.82
12	Ball Valve	2,283,951	1.18
13	Knock-Out Drum (Flash Drum)	140,051	2.29
14	Pressure Safety Valve (PSV)	604,906	1.003

Table 2. Unrepairable component failure rates (Dirik et al., 2022)

No	Components	Probability of Failure (per Hour)
15	Manifold (M)	2.27×10^{-5}
16	Temperature Sensor (TS)	6.39×10^{-6}
17	Thermocouple Sensor	8.56×10^{-6}
18	Pressure Sensor (Electro-Mechanical)	5.75×10^{-6}
19	Level Sensor (conductivity)	5.71×10^{-5}
20	Flow sensor	4.95×10^{-6}

As presented in Figure 2, the first step of the research work was initiated by identifying the data analysis requirements within the system. Failure data for some components were derived from the OREDA, Failure Rate Data in Perspective (FARADIP.THREE, 2015; Center for Chemical Process Safety, 1989), European Industry Reliability Data Bank (EIREDA) (Procaccia et al., 1997), and SINTEF (n.d.).

Figure 2 can be summarized as follows: First, MCS was implemented using Visual Studio C++ coding for each component's logical relationships and statistical distribution. The C++ code generates the results and then saves them into an Excel (.csv) file to detect the timing of system failure. These features are used to capture the failure sequence.

Second, the Method of moments was used to calculate the total system Weibull parameters, using an existing formulation and goal Seek function capability in Excel. This result was simulated and then presented reliably as system graphics. MCS not only can estimate the failure but also provides a platform for the visualization of sequential failure. The μ and σ values were transformed using the equations ln μ and ln (σ 2+ μ 2). After algebraic manipulation, each 2lnα

IDRiM (2025) 15 (1) **ISSN: 2185-8322**
DOI10.5595/001c.129129

was set equal to zero. All formulas were implemented in Excel (e.g., using What-if Analysis and the Goal Seek function) in order to estimate the Weibull parameters.

The data of seasonal lightning strikes and flooding patterns were secondary data sets also analyzed. The general procedures are presented in the flowchart shown in Figure 2.

The final step was to implement the failure distribution parameters for key components using visual studio C# codes. Each iteration was considered as a one-hour system snapshot, which was listed in an Excel file so that temporal and statistical calculations could be performed. Lightning–flooding correlations were converted into system codes. Each iteration determined the lowest limit of lightning density which may result in flooding in Selangor prefecture, Malaysia.

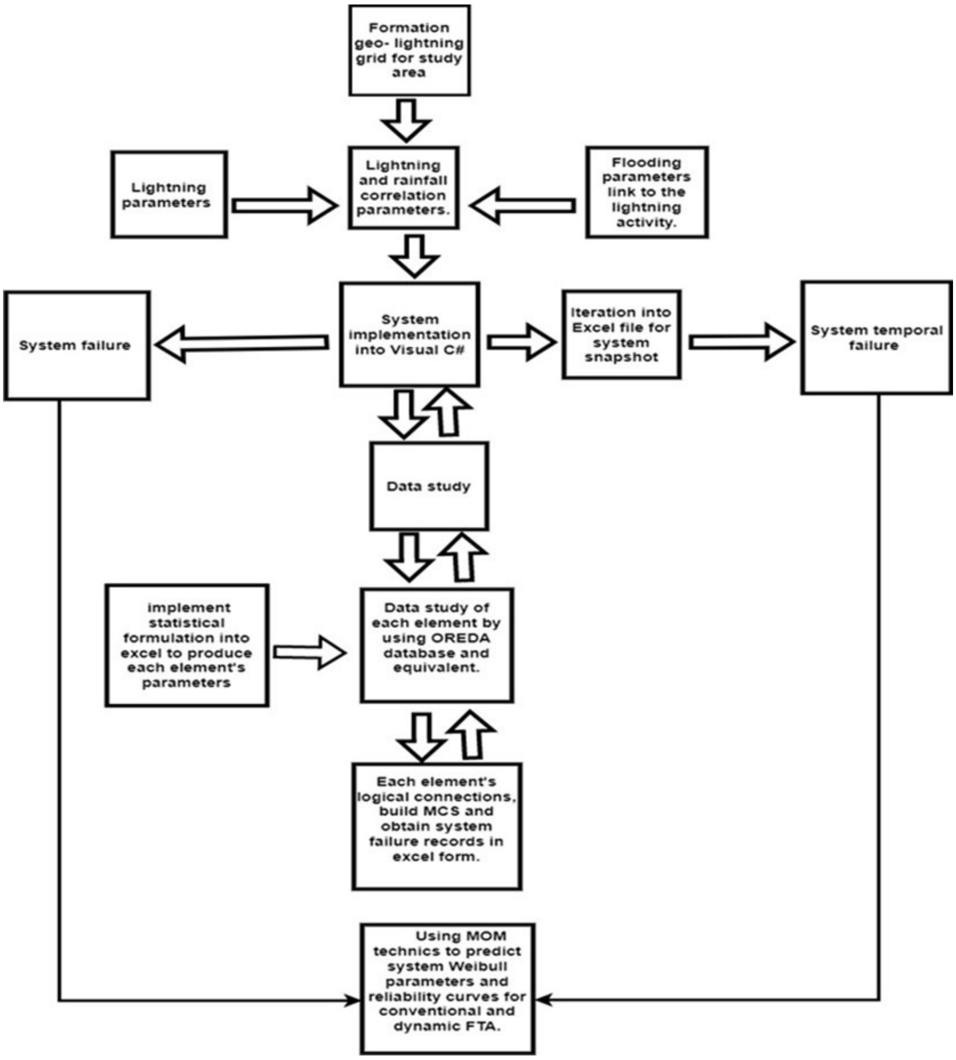

Figure 2. Flowchart of the developed methodology

Figure 3 summarizes the main idea process underlying TFT. Flooding may occur in the target area if the number of seasonal lightning strikes exceeds the minimum limit. Consequently, flooding can be expected to occur; this sequence is called a temporal failure. The second

DOI10.5595/001c.129129

scenario is that a lightning strike causes sensor failure first, after which further lightning strikes occur; this is called a system failure. These logical ideas form the dynamic part of the risk analysis. The conventional risk analysis part is presented at the end of the flowchart.

MCS simulates real situations by generating random numbers for seasonal lightning data, together with component failure and failure timing data, which are crucial for TFTA.

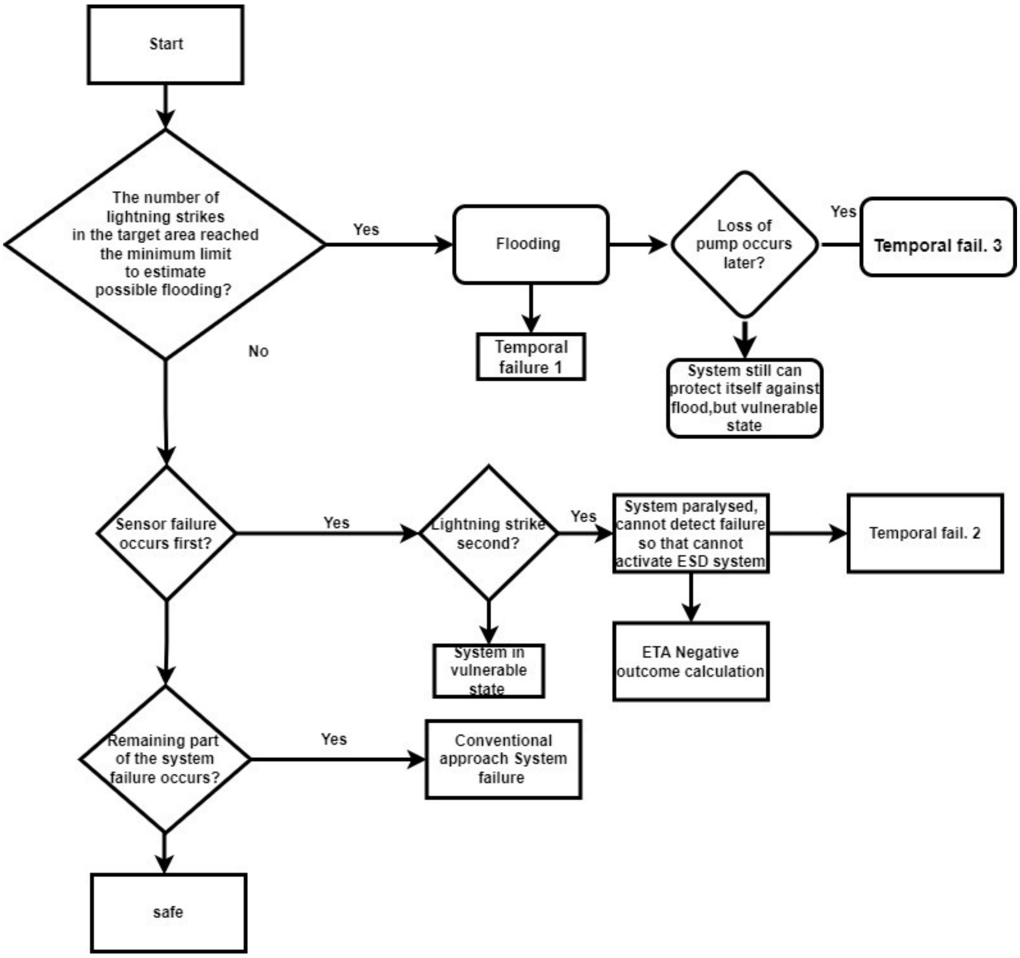

Figure 3. TFT logic flowchart

The following step is to conduct detailed sequential procedures to quantify the risk and estimate the system reliability and failure statistics using the Weibull parameters; in particular, the Weibull distribution was used to describe the failure frequency distribution. We employed the method of moments (MoM) to estimate the Weibull parameters according to the best fit of the data and a method of estimation for population parameters. After the simulation, nine sampling points were used for each specific time interval, and the method of statistical moments technique was conducted using Excel. In this way, a system reliability curve could be obtained.

It can be noted, from the results, that the first failure occurred within the first 10,000 hours. Each failure timing is the mean of ten different trials. The considered vaporizer unit consisted of various key components, such as valves, detectors, and pumps, with six valves present in the system. A combination of the voting OR gate (5/7) failures were considered as system failures.

The last step is employing ETA to visualize and quantify the negative consequence that is system paralysis ends up with a catastrophe.

2.1 Method of Moment Definition

One of the popular methods for estimating the times-to-failure in continuous failure testing on mechanical or electronic equipment is the Weibull distribution. In order to estimate the parameters of a Weibull distribution, it is studied the performance of the method of moments. Finding a Weibull distribution with a given mean, variance, and location parameter is frequently required. The standard method includes calculating the parameters using an iterative numerical process via Visual Studio C#, to estimate the greatest probability of the gamma parameters.

While Γ is a Gamma function.
The (three-parameters) Weibull distribution is:

$$F(x) = 1 - \exp\,[-a(x-c)^b],\ c \leqq x < \infty, \tag{1}$$

with density

$$f(x) = ab(x-c)^{\mathrm{b}-1}\big[-a(x-c)^{\mathrm{b}}\big]. \tag{2}$$

The mean and variance are:

$$\begin{aligned} \mu &= c + \mathrm{a}^{-1/\mathrm{b}}\Gamma(1+1/b) \\ \sigma^2 &= \mathrm{a}^{-2/\mathrm{b}}[\Gamma(1+2/b) - \Gamma^2(1+1/b)] \end{aligned} \tag{3}$$

The moment estimators of a and b (c assumed known) are obtained by solving Equations (3) for a and b, using the sample mean and variance. One way of solving (3) is:

(i) Solve for b

$$\Gamma(1+2/b)/\Gamma^2(1+1/b) - 1 = [\sigma/(\mu-c)]^2 \tag{4}$$

(ii) Compute a from

$$a = [\Gamma(1+1/b)/(\mu-c)]^{\mathrm{b}} \tag{5}$$

Equation (4) may be solved approximately using any of a number of standard iterative root-finding procedures. (Approximation for b as a function of $\sigma/(\mu-c)$ is used.)

2.2 Weibull Parameter Estimation (Dirik et al., 2022)

An approach for the estimation of Weibull parameters has previously been proposed by the authors (Dirik et al., 2022), as follows:

The Weibull parameters estimation is determined using the following equations:

$$\sigma^2 = \alpha^2\,\Gamma(1 + 2/\beta) - \mu^2,\ \mu = \alpha\Gamma(1 + 1/\beta) \quad (6)$$

$$\ln \mu = \ln \alpha + \ln \Gamma(1 + 1/\beta),\ \ln(\sigma^2 + \mu^2) = 2 \ln \alpha + \ln \Gamma(1 + 2/\beta) \quad (7)$$

where μ is the mean and σ is the standard deviation, and the gamma function is denoted by Γ. The values for μ and σ can be estimated using Equation (6).

The μ and σ values are transformed by the formulas $\ln \mu$ and $\ln(\sigma^2 + \mu^2)$. After algebraic manipulation, each $2\ln\alpha$is equal to zero. Each formula was implemented using Excel What-if Analysis, allowing for estimation of the Weibull parameters.

Equation (8) was then rearranged to yield. The value for β in equation (9) was solved using a simultaneous equation that generates values for β in the function Γ, while the value for α was solved using equation (9):

$$\ln \Gamma(1 + 2/\beta) - 2 \ln \Gamma(1 + 1/\beta) - \ln(\sigma^2 + \mu^2) + 2 \ln \mu = 0 \quad (8)$$

$$\alpha = x/(\Gamma(1 + 1/\beta)) \quad (9)$$

2.3 Geo-Lightning Grid Approach for Obtaining Seasonal Lightning Strike Data

The geo-lightning grid was based on a geographical information system and consisted of cells with defined edges. The main SCV unit in Figure 4 (yellow point) was located in the middle of the complex, surrounded by five other buildings and pipelines.

The geo-lightning grid presents the number of strikes inside the area of each cell for a defined range of time, with values derived from Lightning Imaging Sensor Instrument Team and the Global Hydrology Resource Center (GHRC; NASA, US Government).

The center of the black frame presented in Figure 5 is the target area, which is subject to dramatic flooding risk. Sungai Udang LNG Terminal facility is located in North Malaysia, with relatively higher probabilities of lightning and flooding. The ten year- average number of lightning strikes was obtained from the website (Figure 5, calculated as a monthly average).

Each monthly average was included into the simulation codes to capture the lightning and flooding probabilities.

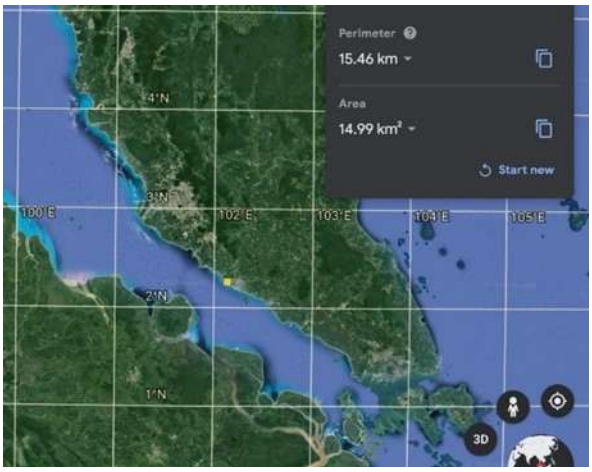

Figure 4. Location of Sungai Udang LNG Terminal, Image courtesy Google Earth

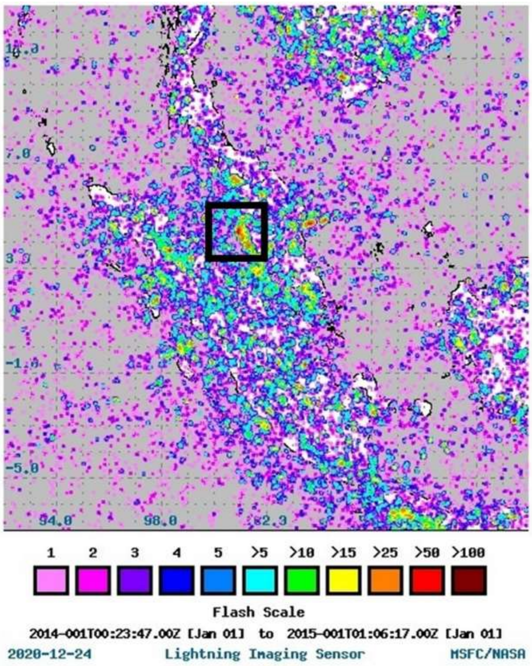

Figure 5. Lightning flash density map for the area of interest, Image courtesy NASA.

3. CASE STUDY: LNG VAPORIZER UNIT

The diagram of an SCV will be analyzed as a case study. It is designed to generate the heat needed to vaporize the LNG flow, as shown in Figure 6 (Qi et al., 2016). In the SCV, the water bath covers the combustion furnace and heat exchange coil. At the base of the water bath, gas from the furnace is forced into the water through the flue gas pipe. Thus, the heat exchange coil can almost fully absorb the combustion heat of natural gas through the water bath. Flow sensors on the inlet and outlet lines can sound low flow alarms in the control room, while temperature sensors monitor the temperature of the bath water, which can also activate an alarm under certain conditions. SCVs provide various advantages, such as rapid operations (start-up and shut down) and the prevention of ice build-up on tubes. Furthermore, the heat exchange medium is water, which is safer than other fluids (Qi et al., 2016).

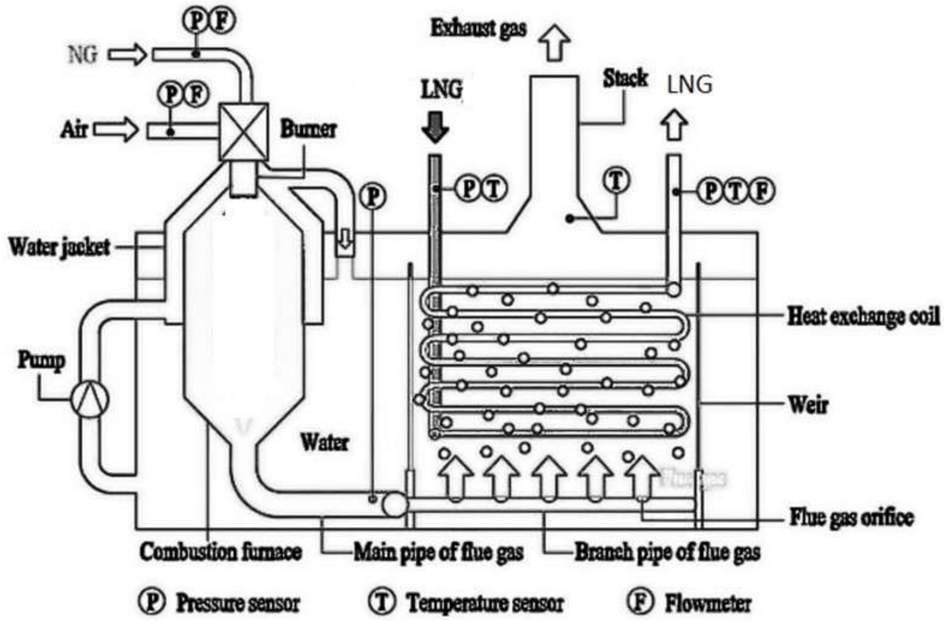

Figure 6. Structure of the LNG SCV unit: Element of the SCV (P, pressure sensor; T, temperature sensor; F, flow sensor)

The logical configuration of SCV failure is shown in Figure 7, comprising four different parts (as groups of temporal or conventional events): Temporal failure 1, Temporal failure 2, Temporal failure 3, and conventional SCV failure. Primary events, namely lightning, flooding, sensor failure, and loss of pump, were identified as the root causes leading to the operational failure of the SCV. In addition, lightning and flooding were considered basic external events, which may sequentially lead to operational failure. The sequential failure events of the vaporizer are defined as follows:

Temporal failure 1: A lightning strike has enough intensity to estimate possible flooding for the target area. The number of lightning strikes and flooding are correlated, and a system failure occurs.

Temporal failure 2: Sensor failure occurs first, and lightning strikes second. As long as the sensor fails, the system cannot detect the failure and cannot activate ESD.

Temporal failure 3: Flooding occurs first, leading to a loss of pump. This results in total system failure. Failure of sensors in the chemical industry may lead to failure of the overall system, as the system cannot take action against the loss and, consequently, damage to the environment or the death of employees may occur. These dangers exist not just due to the chemicals being handled, but also to the violent force that may occur if there is an explosion. Failure of sensors may prevent the safety barrier from detecting any deviation in system parameters. The loss of sensor hierarchy is shown in Figure 8.

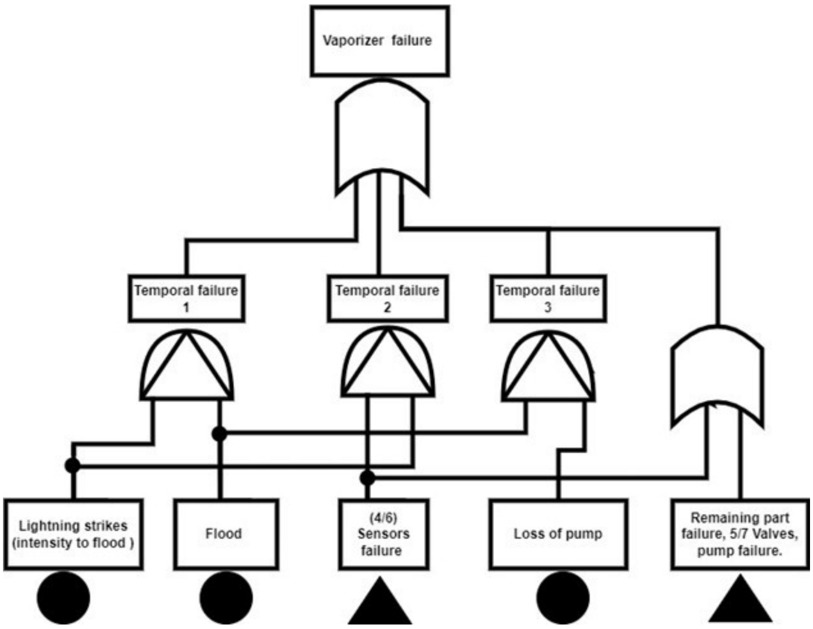

Figure 7. SCV failure in TFT hierarchy

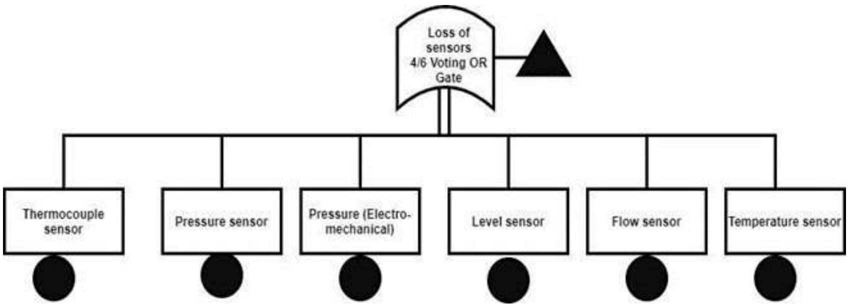

Figure 8. Sensor failure hierarchy

The remaining part failure detailed in Figure 9 consists of two major parts: Failures associated with the valves and those associated with the centrifugal pumps. Six valves are used in the system. The failure of valves is described by the voting OR gate, in which the system will fail when the k/n value is 5/7.

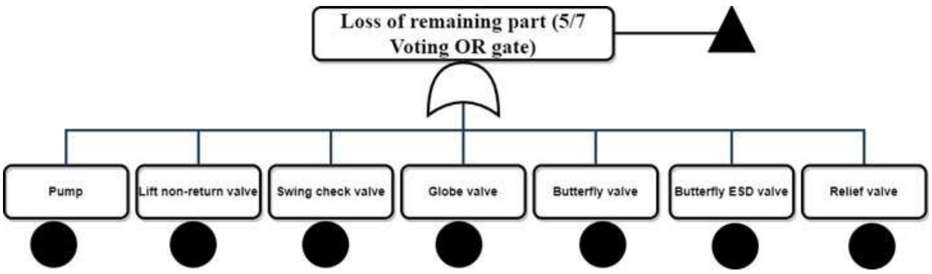

Figure 9. Remaining part failure hierarchy

4. RESULTS AND FINDINGS

Natural events were integrated into the reliability analysis through the MCS, allowing graphical results to be obtained. Based on the MCS estimates, the sequential failures occurred as frequently as 27 times, whilst the conventional failure estimate indicated that such an event only occurred 2 times over the operational period of 32.4 years. From Table 3, it can be noted that Sequential failure 2 contributed significantly to the overall failure probability of the unit. Sequential failure 2 alone occurred around 14 times over 300,000 iterations. The structure of the temporal failure 2 may lead to system paralysis, which means that the system cannot detect the failure and then can not activate the ESD system. Sequential failure 1, which is associated with flooding, only nine times occurred. Notably, flooding has the capability for serious consequences that are more severe than those in other events, as flooding may lead to drift debris, rigid items, or floating debris, increasing the lateral force s on a total unit (Seo et al., 2020), Sequential failure 3 which is associated with flooding and loss of pump contributed only four times, giving the lowest percentage of system failure probability. Excessive water may cause power outages or damage, leading the pumps to not operate properly, which is the most common cause of pump-related damage. Assuming the installation of this facility in the Selangor area, it will encounter an average of 19 lightning strikes per hour; however, it has been concluded that only negatively charged lightning may lead to possible hazards (Hassan, et.al 2011), regarding the vaporizer.

Table 4 presents the time-to-failure for the LNG SCV. As a result of MCS, system failure time samples could be tabulated. Eleven samples of failure timing were taken to obtain the Weibull parameters for the vaporizer system, where the Method of Moments was used to estimate the Weibull parameters.

Based on the MCS estimation conducted in this study, the scale (α, h) and shape (β) parameters of the Weibull distribution for the SCV were 76,898.13 h and 1.148517, respectively.

We could determine the Reliability and Reliable Life of the vaporizer system; for example, if the reliability of a unit at 42,000 h is 60%, then the Reliable Life for 60% Reliability would be 42,000 h.

SCV sequential (temporal) failure consists of three parts: namely, sensor failure, external events, and loss of discharge (pump). The reliability graph for the onshore terminal SCV is provided in Figure 11, for which dynamic simulation based on working time was conducted. Through the simulation analysis detailed above, the relevance of the system components to the overall reliability was further studied. As a result, the combined effect of flooding and lightning on the total system failure is depicted on the reliability graph.

Table 3. Vaporizer sequential failure probability table (/hour)
(LOD, Loss of Discharge; LS, Lightning Strike; SF, sensor failure)

Events	Sequential Fail. 1	Sequential Fail. 2	Sequential Fail. 3	Conventional Failures
	LS◄FL	SF◄LS	Fl◄LOD	Conventional failure
	3×10^{-5}	4.6×10^{-5}	1.3×10^{-5}	6.6×10^{-6}
Percentage in total failures (%)	31.25	47.9	13.5	6.8
Total frequency		9.6×10^{-5} (/h)		

Table 4. Time to system failure for 11 samples

Sample	1	2	3	4	5	6	7	8	9	10	11
Time to failure (h)	9949	25,533	61,239	34,045	198,565	13,253	77,247	37,928	69,324	96,681	181,564

5. ETA EVALUATION AND FINDINGS

Sensor system and lightning strike probability depend on ESD system reliability. Weibull distribution behavior was assumed for the system's failure frequency as the ESD system's components are made up of both repairable and non-repairable equipment. Equation displays the associated parameters, which were determined by estimating the system's dependability function using the Weibull distribution method. After simulation,

$$. \alpha=21761, \beta=0.7, R(t) = e^{-\left(\frac{8760}{21761}\right)^{0.7}}, \quad t > 0, \qquad R=0.60 \tag{10}$$

is obtained.

The reliability of the parallel redundant system (RR) for the ESD was recalculated according to the following:

$$R_R(D) = R_1+R_2-R_1R_2 = 0.6+0.6 - 0.6*0.6$$

$$=1.2-0.36=0.84 \tag{11}$$

The probability of failure in demand (PFoD) for the redundancy system for the ESD (PR(D)') is 1- 0.84 = 0.16.

An instantaneous release that is ignited immediately in a stationary installation has a chance of 0.7 and can result in BLEVE (Boiling liquid expanding vapor explosion) and a fireball, or

IDRiM (2025) 15 (1) **ISSN: 2185-8322**
DOI10.5595/001c.129129

early pool of fire. It is possible to assume that a delayed ignition of an unconfined vapor cloud may be treated as two distinct events: a pure explosion with a probability of 0.6 and 0.4, respectively, and a flash fire that might possibly involve a pool fire, depending on the circumstances (van den Bosch & Weterings, 2005), presented on Figure10 and Table 5. Simply wind direction ¼ is taken. Temporal failure 2 is taken as an initiator.

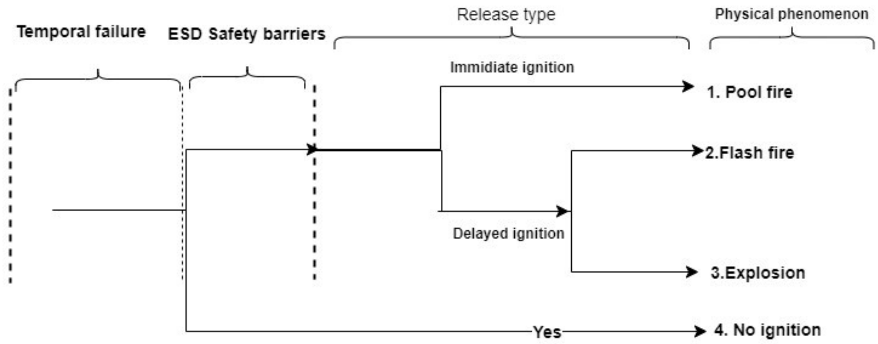

Figure 10. ETA configuration

Table 5. ETA frequency calculation table

CONSEQUENCE	IMMEDIATE IGNITION (PER HOUR)	DELAYED IGNITION (PER HOUR)
Pool fire	$4.05x10^{-7}$	-
Flash fire	-	$3.5x10^{-6}$
Explosion	-	$2.34x10^{-6}$
Wind direction	25%	25%
Total failure frequency	$1.56x10^{-6}$	

While total system failure frequency is taken for ETA negative consequence probability, it becomes $3.25x10^{-6}$ (/h)

6. CONCLUSIONS

This study aimed to conduct a total system failure simulation for an SCV in the chemical process safety area, allowing for the assessment of the system's reliability. Sixty percent of the reliability value takes 42.000 hours, approximately five years in the total period of time, as can be seen in Figure 11. It is important to note that preventive actions are not considered.

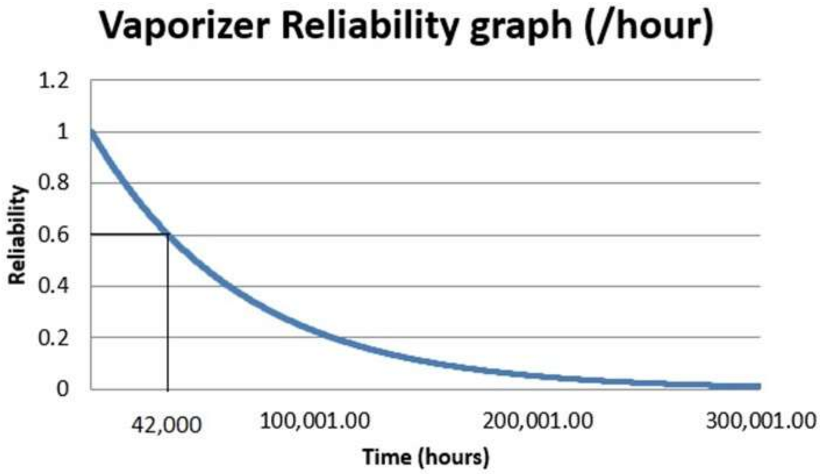

Figure 11. Vaporizer reliability graph: Reliability vs Time (hours). Note: 300,000 hours

We proposed a novel dynamic risk analysis approach that combine two natural phenomena (i.e., lightning and flooding) into the temporal fault tree analysis, as well as integrating the temporal correlation between these phenomena. Notably, conventional methods are not capable of detecting such failures. The obtained reliability and Weibull parameters of the system were more precise and closer to real system parameters.

This idea can be further applied to the climatology and hydrology fields, which are beyond the scope of this study. Our case study was applied to Selangor prefecture in Malaysia, but this unique approach can be applied to other locations that are prone to natural disasters (i.e., tsunamis, hurricanes, and earthquakes).

ETA is a strong instrument that will pinpoint every outcome of a system that has a chance of happening following an initiating event as results of the simulation and relevant calculation frequency of the catastrophe consequence for temporal failure 1.56x10-4 (/h) are obtained.

ACKNOWLEDGMENTS

Author Contributions: CD: Writing—review and editing, Writing—original draft, Investigation, Formal analysis, Methodology, Conceptualization; DRAB: Supervision, Project administration, Funding acquisition; M.b.A.R.: Validation; NNLNI: Data curation. All authors have read and agreed to the published version of the manuscript.

Funding: This research received no external funding

Institutional Review Board Statement: Not applicable

Informed Consent Statement: Not applicable

Data Availability Statement: Data is Available Upon Request.

DOI10.5595/001c.129129

Declaration of competing interest: The authors declare that they have no known competing financial interests or personal relationships that could have appeared to influence the work reported in this paper.

REFERENCES

Ab-Kadir, M. (2016). Lightning severity in Malaysia and some parameters of interest for engineering applications. *Thermal Science*, *20*(suppl. 2), 437–450. https://doi.org/10.2298/TSCI151026028A

Ahmad, M. R., Baharin, S. A. S., Yusop, N., Esa, M. R. M., & Sidik, M. A. B. (2022). Occurrence of Positive Cloud-to-Ground Lightning During Flash Flood in Malacca. *2022 IEEE International Conference in Power Engineering Application (ICPEA)*, 1–3. https://doi.org/10.1109/ICPEA53519.2022.9744678

Center for Chemical Process Safety. (1989). *Guidelines for process equipment reliability data with data tables.* aiche.org.

Dirik, C., Awang Biak, D. R., Abdul Razak, M., & Nik Ibrahim, N. N. L. (2022). Externally initiated event in sequential risk assessment for the onshore LNG marine loading arm unit. *Journal of Loss Prevention in the Process Industries*, *75*, 104717. https://doi.org/10.1016/j.jlp.2021.104717

FARADIP.THREE. (2015). *(Version 8)*. Technis. www.wilderisk.co.uk

Gungle, B., & Krider, E. P. (2006). Cloud-to-ground lightning and surface rainfall in warm-season Florida thunderstorms. *Journal of Geophysical Research*, *111*(D19), D19203. https://doi.org/10.1029/2005JD006802

Han, C.-L., Sun, H.-Q., & Li, Z.-Y. (2018). Thermal performance analysis and optimization design for LNG submerged combustion vaporizer. *Cryogenics*, *95*, 47–56. https://doi.org/10.1016/j.cryogenics.2018.08.008

Hassan, M. K., Rahman, R.A., Soh, A. and Kadir, Z.A. (2011). Lightning strike mapping for Peninsular Malaysia using artificial intelligence techniques, *Journal of Theoretical and Applied Information Technology*, *34*(2), 202–214.

Ismail, M. S. N. (2019). THE CHARACTERISTICS OF ROAD INUNDATION DURING FLOODING EVENTS IN PENINSULAR MALAYSIA. *International Journal of GEOMATE*, *16*(54). https://doi.org/10.21660/2019.54.4827

Johari, D., Aiman Misri Amir, M. F., Hashim, N., Baharom, R., & Haris, F. A. (2021). Positive Cloud-to-Ground Lightning Observed in Shah Alam, Malaysia based on SAFIR 3000 Lightning Location System. *2021 IEEE International Conference in Power Engineering Application (ICPEA)*, 178–182. https://doi.org/10.1109/ICPEA51500.2021.9417761

Mannan, S., & Mannan, M. S. (2012). *Lee`s Loss Prevention in the Process Industries: Hazard Identification, Assessment And Control: Fourth Edition*. 2012 Elsevier Inc.

Mohammad, S. A., Esa, M. R. M., Abdul-M, Z., Ahmad, M. R., Yusop, N., York, S. B., Periannan, D., Sabri, M. H. M., Baharin, S. A. S., Sidik, M. A. B., Nawawi, Z., Jambak, M. I., & Lu, G. (2019). Radar Analysis of a Tropical Hailstorm Associated with Lightning Flash Rate. *2019 International Conference on Electrical Engineering and Computer Science (ICECOS)*, 141–144. https://doi.org/10.1109/ICECOS47637.2019.8984453

DOI10.5595/001c.129129

Papadopoulos, A., Serpetzoglou, E. & Anagnostou, E. N. (2009). Evaluating the impact of lightning data assimilation onmesoscale model simulations of a flash flood inducing storm. *AtmosphericRes*, *94*, 715–725.

Pan, J., Wang, J., Tang, L., Bai, J., Li, R., Lu, Y., & Wu, G. (2020). Numerical investigation on thermal-hydraulic performance of a printed circuit LNG vaporizer. *Applied Thermal Engineering*, *165*, 114447. https://doi.org/10.1016/j.applthermaleng.2019.114447

Price, C., Yair, Y., Mugnai, A., Lagouvardos, K., Llasat, M. C., Michaelides, S., Dayan, U., Dietrich, S., Galanti, E., Garrote, L., Harats, N., Katsanos, D., Kohn, M., Kotroni, V., Llasat-Botija, M., Lynn, B., Mediero, L., Morin, E., Nicolaides, K., … Ziv, B. (2011). The FLASH Project: using lightning data to better understand and predict flash floods. *Environmental Science & Policy*, *14*(7), 898–911. https://doi.org/10.1016/j.envsci.2011.03.004

Procaccia, H., Aufort, P., & Arsenis, S. (1997). The European Industry Reliability Data Bank EIReDA. In *Advances in Safety and Reliability*. https://doi.org/10.1016/b978-008042835-2/50204-6

Qi, C., Wang, W., Wang, B., Kuang, Y. & Xu, J. (2016), Performance analysis of submerged combustion vaporizer, *Journal of Natural Gas Science and Engineering*, *31*, 313–319.

Ricci, F., Casson Moreno, V., & Cozzani, V. (2021). A comprehensive analysis of the occurrence of Natech events in the process industry. *Process Safety and Environmental Protection*, *147*, 703–713. https://doi.org/10.1016/j.psep.2020.12.031

Rukke, S., & Katchmar, P. (2016). *Failure Investigation Report – Liquefied Natural Gas (LNG) Peak Shaving Plant, Plymouth, Washington*. US Department of Transportation. file:///C:/Users/fizik/OneDrive/Desktop/son2/FIR_and_APPENDICES_PHMSA_WUTC_Williams_Plymouth_2016_04_28_REDACTED.pdf

Seo, S., Park, Y.G. and Kim, K. (2014). Tracking flood debris using satellite-derived ocean color and particle-trackingmodeling, *Marine Pollution Bulletin, 161*(Part A), 111828.

SINTEF. (n.d.). SINTEF. https://www.sintef.no/

Sofia, G., & Nikolopoulos, E. I. (2020). Floods and rivers: a circular causality perspective. *Scientific Reports*, *10*(1), 5175. https://doi.org/10.1038/s41598-020-61533-x

Winsemius, H. C., Aerts, J. C. J. H., van Beek, L. P. H., Bierkens, M. F. P., Bouwman, A., Jongman, B., Kwadijk, J. C. J., Ligtvoet, W., Lucas, P. L., van Vuuren, D. P., & Ward, P. J. (2016). Global drivers of future river flood risk. *Nature Climate Change*, *6*(4), 381–385. https://doi.org/10.1038/nclimate2893

Price, C., Yair, Y., Mugnai, A., Lagouvardos, K., Llasat, M. C., Michaelides, S., Dayan, U., Dietrich, S., Galanti, E., Garrote, L., Harats, N., Katsanos, D., Kohn, M., Kotroni, V., Llasat-Botija, M., Lynn, B., Mediero, L., Morin, E., Nicolaides, K., … Ziv, B. (2011). The FLASH Project: using lightning data to better understand and predict flash floods. *Environmental Science & Policy*, *14*(7), 898–911. https://doi.org/10.1016/j.envsci.2011.03.004

Tapia, A., Smith, J. A., & Dixon, M. (1998). Estimation of Convective Rainfall from Lightning Observations. *Journal of Applied Meteorology*, *37*(11), 1497–1509. https://doi.org/10.1175/1520-0450(1998)037<1497:EOCRFL>2.0.CO;2

Wingender, H. J. (1986). *Reliability Data Collection and Use in Risk and Availability Assessment*. Springer Berlin Heidelberg. http://link.springer.com/10.1007/978-3-642-82773-0

Zorilla, L. A. (2011). Geo-Lightning grid based on a Geographical Information System, to Improve poles distribution network designs, prioritize maintenance and boost the power system reliability. *" IX Latin American Robotics Symposium and IEEE Colombian Conference on Automatic Control, 2011 IEEE, 2011, Pp. 1-6,* 1–6. https://doi.org/10.1109/LARC.2011.6086861